B2.7 MOVPE of GaN and related compounds

J.M. Redwing and T.F. Kuech

August 1998

A INTRODUCTION

Metalorganic vapour phase epitaxy (MOVPE) has developed over the past ten years into the premier technique for the epitaxial growth of the group III nitrides. Since GaN or AlN substrates have not been generally available, GaN epitaxy has been carried out on highly lattice mismatched substrates, such as silicon [1,2], sapphire [2,3] and GaAs [3,4]. Advances in growth technology, in particular the use of thin AlN [5] and GaN [6] buffer layers on sapphire substrates, produced dramatic improvements in material quality and led to the development of n-type and p-type doping processes [7,8] as well as the growth of (Al,Ga,In)N compounds and heterostructures [9-11]. The success of MOVPE in the production of high brightness light emitting diodes [12] and short wavelength injection lasers [13] has resulted in a rapid expansion of research and development in this materials system.

In spite of the enormous potential of MOVPE for the production of commercial nitride devices, little is known about the fundamental chemistry and transport processes that govern the GaN growth process. Strong gas phase reactions occur at room temperature between the metalorganic sources, typically trimethylgallium (TMGa) or triethylgallium (TEGa), and ammonia (NH_3) [14-17]. As a result, it is necessary to introduce the group III and V sources into the reactor through separate inlet tubes and mix the reactants at elevated temperatures near the growth surface. The optimum parameter space for group III nitride growth is typically determined empirically in a given reactor configuration. In general, high growth temperatures (>1000°C), high V/III ratios (>1000) and high gas velocities are required to produce continuous GaN films with a low background n-type doping and a high electron mobility [18]. Conditions are similar for the growth of AlGaN alloys, although the growth rate of AlN is typically much lower than that of GaN. Reduced temperatures (<800°C) and very high V/III ratios (>10000) are required for the growth of InGaN alloys [19]. In addition, it is difficult to grow high In-content InGaN layers in a hydrogen carrier gas [20]; therefore, nitrogen is favoured as the carrier gas when growing InGaN heterostructures [12].

Recent studies have begun to focus on the development of a comprehensive growth model to explain these effects [21-23]. Several extensive reviews have previously been written discussing the growth methods and properties of (Al,In,Ga)N layers grown by MOVPE [24-26]. This Datareview, therefore, focuses on the chemical aspects of GaN growth, reviewing the current understanding of the gas phase chemistry, surface reactions and transport processes that govern the growth of GaN and its related alloys, AlGaN and InGaN.

B MOVPE GROWTH PROCESS

Insight into the fundamental mechanisms controlling the MOVPE growth of GaN and related alloys can be obtained by studying the effect of external parameters such as substrate temperature and source gas flow rate on growth rate and composition. This type of investigation has been carried out extensively for the group III arsenides and phosphides. In general, a study of growth rate dependencies can be used to assess the extent of gas phase pre-reaction of sources as well as to distinguish between growth processes that are limited by mass transport, kinetics or thermodynamics.

B1 Growth Efficiency

A comparison of the growth efficiency of GaN, defined as the experimentally measured growth rate divided by the molar flow rate of the group III sources into the reactor, with that of other materials systems offers insights into the relative importance of chemical reactions occurring upstream of the growth surface. Stringfellow has listed the growth efficiency of various chemical precursors in the MOVPE growth of GaAs and InP-based compounds [27]. High growth efficiencies are typically reported for those growth sources that do not undergo extensive gas phase reactions. The growth of GaAs from TMGa and AsH_3, for example, usually exhibits a growth efficiency of about 1000 - 10000 μm/mol of reactant. In contrast to this, growth efficiencies in the range of 500 - 1000 μm/mol are obtained for the growth of InP due to a gas phase reaction between triethylindium (TEIn) and PH_3.

TABLE 1 contains a collection of growth efficiencies for GaN [28-35], AlGaN [35-37] and InGaN [12,19,30] reported in the literature for a variety of growth conditions and reactor geometries. GaN exhibits moderate growth efficiencies in the range of 600 - 6000 μm/mol. Reported growth efficiencies for $Al_xGa_{1-x}N$ are lower (<2000 μm/mol) and, in general, decrease with increasing Al fraction (x) as shown in FIGURE 1 [35]. AlN growth efficiencies are also strongly dependent on reactor pressure. Chen et al [28] reported a growth efficiency of 1000 μm/mol for AlN grown at 85 torr dropping to zero for atmospheric pressure growth. $In_yGa_{1-y}N$ alloys have very low growth efficiencies (<300 μm/mol) due to the high TMIn flow rates which are required to incorporate In into the material at elevated temperature.

TABLE 1 Reported growth efficiencies (Rg/F(III)) for GaN, AlGaN and InGaN.

Materials system	Sources	x or y	Rg/F(III) (μm/mol)	Reactor pressure (torr)	Substrate temperature (°C)	V/III ratio	Ref
GaN	TMGa + NH_3		1.0×10^3	85	700 - 1000	1350	[28]
	TMGa + NH_3		9.5×10^2	780	500 - 1000	1350	[28]
	TMGa + NH_3		5.8×10^3	760	1090	4780	[29]
	TMGa + NH_3		2.5×10^3	760	1020	6017	[30]
	TMGa + NH_3		1.4×10^3	760	1000	3760	[31]
	TEGa + NH_3		6.0×10^2	45	950	2460	[32]
	TMGa + NH_3		1.0×10^3	57	1040	3950	[33]
	TEGa + NH_3		6.4×10^2	60	1030	4077	[34]
	TMGa + NH_3		2.2×10^3	100	1100	4000	[35]
$Al_xGa_{1-x}N$	TMGa + TMAl + NH_3	0.33	1.5×10^3	100	1100	4000	[35]
	TMGa + TMAl + NH_3	0.58	1.0×10^3	100	1100	4000	[35]
	TMGa + TMAl + NH_3	1.0	1.0×10^3	85	500 - 800	1350	[28]
	TMGa + TMAl + NH_3	1.0	0.0	780	500 - 1000	1350	[28]
	TMGa + TMAl + NH_3	~0.20	2.6×10^2	70	1025	286	[36]
	TEGa + TEAl + NH_3		1.4×10^3	76	1000	6770	[37]
$In_yGa_{1-y}N$	TMIn + TMGa + NH_3	0.14 - 0.20	1.3×10^2	760	800 - 830	6250	[30]
	TMIn + TMGa + NH_3	0.06	1.9×10^2	760	800	9025	[29]
	TMIn + TEGa + NH_3	0.12 - 0.24	2.9×10^2	76	500 - 800	20000	[19]

B2 Parametric Studies

The experimentally measured growth efficiency of GaN as a function of substrate temperature is shown in FIGURE 2 [28,38]. The temperature dependence of GaN growth efficiency is similar to that obtained for GaAs growth [39]. At lower growth temperatures (<600°C), the growth rate increases with substrate temperature, indicative of a kinetically-limited process. A weakly temperature dependent region exists from about 600 to 1000°C, where the diffusion of Ga species to the substrate limits the growth rate. The growth rate in this region exhibits a weak power law dependence on growth

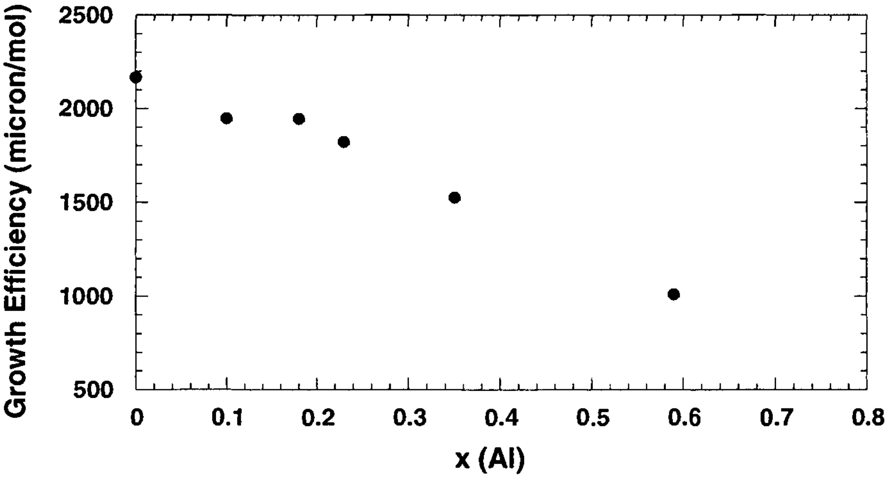

FIGURE 1 Growth efficiency of AlGaN as a function of composition [35]. Reactor pressure = 100 torr, growth temperature = 1100°C, V/III = 4000, TMGa flow rate = 17 μmol/min; TMAl flow rate varies from 0.8 to 17 μmol/min.

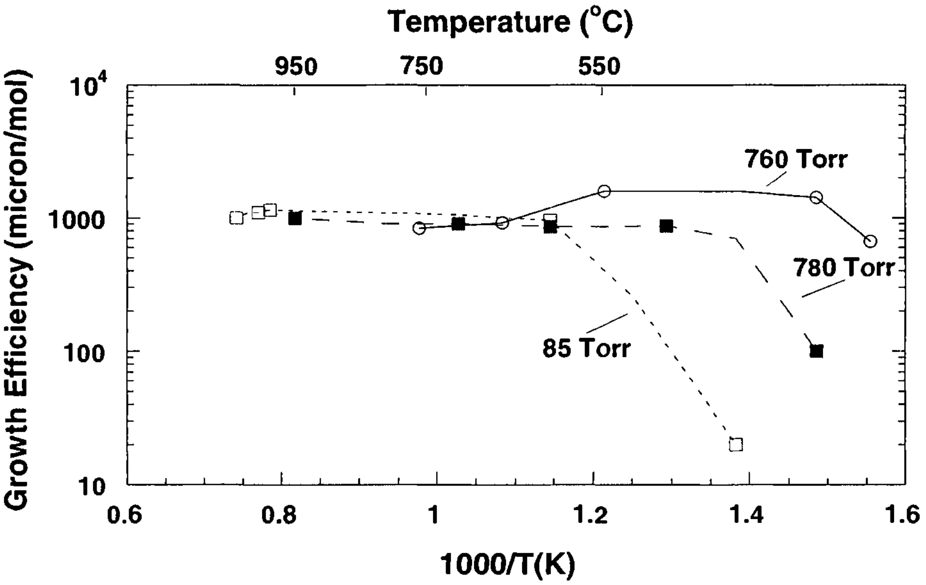

FIGURE 2 GaN growth efficiency as a function of temperature as reported in [28] for reactor pressures of 780 torr (solid squares) and 85 torr (open squares) and in [38] for 760 torr (open circles).

temperature characteristic of a diffusion limited process. GaN is typically grown under these mass transport-limited conditions where the growth rate is proportional to the gas phase mole fraction of TMGa. At temperatures above 1000°C, an increase in temperature results in a slight decrease in growth rate due to either gas phase pre-reactions or desorption of N or Ga species from the surface.

Assuming a simple boundary layer model and a constant inlet flow rate of reactants, the growth rate of GaN is independent of reactor pressure in the mass-transport limited regime. The experimental data shown in FIGURE 2 for various reactor pressures is consistent with this behaviour.

The growth rate of GaN has been reported to be strongly dependent on the V/III ratio used during growth. In the kinetically-limited regime, where the GaN growth rate is temperature dependent, the growth rate decreases with increasing V/III ratio, i.e. with increasing NH_3 flow rate [40,41]. At higher temperatures, Briot et al [41] have observed an increase in the GaN growth rate with increasing NH_3 flux for V/III < 5000 and a decrease in growth rate at higher V/III ratios. A growth mechanism involving competitive adsorption on the surface was proposed to explain the complex dependence on V/III ratio.

The high NH_3 mole fractions used in GaN growth can complicate an analysis of the effect of V/III ratio on growth rate. Since NH_3 typically constitutes a major fraction of the inlet gas stream, a large change in the V/III ratio significantly changes the gas phase properties thereby altering the fluid and thermal profiles in the reactor. Consequently, an increase in the V/III ratio can produce a decrease in GaN growth rate simply by decreasing the flux of reactant species to the growth surface irrespective of a change in gas phase or surface reactions.

B3 AlGaN Alloys

The growth rate and composition dependence of AlGaN growth is strongly dependent on reactor geometry and flow conditions, as a result of the strong gas phase reactions that occur between TMAl and NH_3. Ruffenach-Clur et al [42] have reported that, in the absence of substantial gas phase pre-reactions, the AlGaN solid phase composition is linearly dependent on the gas phase composition with approximately unity slope as shown in FIGURE 3. Sayyah et al [43], on the other hand, reported a sublinear dependence of Al composition and a decrease in growth rate with increasing TMAl flow, similar to the behaviour shown in FIGURE 1. The reported differences in AlGaN growth rate and composition dependence indicate that the MOVPE growth of Al-containing compounds is strongly dependent on reactor geometry, process conditions and gas phase residence time. These growth dependencies are indicative of a process that is controlled by gas phase kinetics.

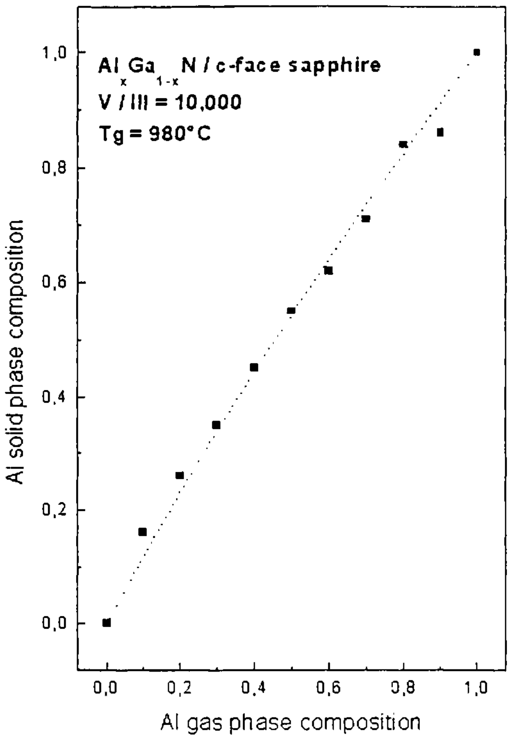

FIGURE 3 AlGaN solid phase composition versus gas phase composition [42].

B4 InGaN Alloys

The growth of InGaN alloys by MOVPE is complicated by several factors including the high volatility of nitrogen over InN and the decrease in In incorporation when hydrogen is used as the carrier gas. The equilibrium vapour pressure of nitrogen over InN is several orders of magnitude higher than for AlN or GaN [44]. As a result, reduced growth temperatures (<800°C) and very high V/III ratios (>10000) are required in order to obtain a sufficient overpressure of nitrogen and maintain a stable growth surface [45]. The solid phase composition of InGaN is strongly dependent on the growth temperature [19,46]. The In fraction decreases sharply with an increase in growth temperature for a given gas phase mole fraction, as shown in FIGURE 4. Higher growth rates also lead to an increase in In composition [47].

Several simple rate models have been proposed to explain InGaN growth behaviour [23,48]. In general, the incorporation of In on the growth surface is viewed as a competition between incorporation and desorption kinetics and the formation of metallic In on the surface. The rate of In desorption increases with increasing growth temperature. The In composition is therefore predicted to increase with decreasing growth temperature and increasing growth rate.

The composition and morphology of InGaN is also strongly dependent on the carrier gas used during MOVPE growth. An N_2 carrier gas reduces the formation of In droplets on the surface and leads to higher In fractions for a given set of growth conditions compared to H_2 [20]. Furthermore, the addition of small amounts of hydrogen to the gas stream during InGaN growth in a nitrogen carrier gas reduces the In composition by as much as 25% [49]. The effect of hydrogen on the incorporation of In is not

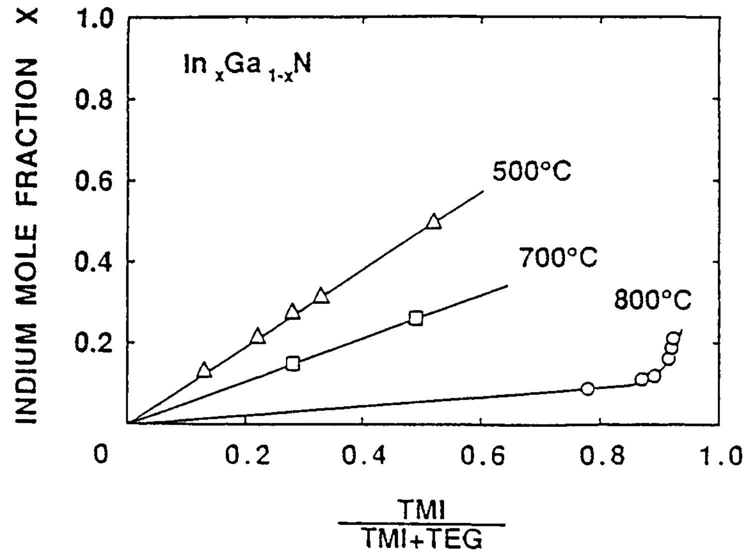

FIGURE 4 InGaN solid phase composition versus gas phase composition as a function of growth temperature [19].

yet fully understood. Hydrogen increases the surface grain size and RMS roughness of GaN buffer layers grown at low temperature [50] and reduces the growth rate of GaN at high growth temperature [51,52]. Consequently, the addition of hydrogen to the growth environment may decrease the lifetime of In species on the growth surface resulting in a reduction in In incorporation. The gas phase transport of In from the growth front is also reduced by the lower gas phase diffusion coefficient of In in N_2 versus H_2. Such reduced gas phase transport leads to an increase in the local In partial pressure near the growth front.

Thermodynamic calculations [53] predict a large miscibility gap for InGaN solid solutions due to the large difference in interatomic spacing between GaN and InN. Phase separation in $In_{0.27}Ga_{0.73}N$/GaN multiple quantum wells grown by MOVPE has been observed after post-growth annealing at 950°C for 40 hr [54]. However, phase separation is generally not observed in 'as grown' InGaN heterostructures and In concentrations up to x = 0.80 have been grown without evidence of immiscibility [55].

C GROWTH CHEMISTRY

The gas phase reactions of TMGa and NH_3, individually, are relatively well understood. The pyrolysis of TMGa in H_2 has been widely studied [56,57], and consists of the step-wise removal of methyl groups. Under similar thermal conditions, NH_3 is quite stable in the gas phase [58] and heterogeneous reactions are considered to be the primary decomposition pathway [59].

In combination, TMGa, a Lewis acid, and NH_3, a Lewis base, can form intermediate coordination compounds at low temperatures. The gas phase reactions of TMGa and NH_3 at low temperatures have been reported by several groups [15-17]. At temperatures <150°C, TMGa and NH_3 react rapidly to form the adduct trimethylgalliummonamine (TMGa:NH_3), as described in EQN (1):

$$(CH_3)_3Ga + NH_3 \leftrightarrow (CH_3)_3Ga{:}NH_3 \qquad (1)$$

Trimethylgalliummonamine has a moderate melting point of 31°C, and a vapour pressure of about 1 torr at room temperature [60]. The estimated and measured strength of the adduct bond are 21.1 kcal/mol and 18.5 kcal/mol, respectively [61].

Studies [61,62] have shown that at ~90°C, the adduct reacts to form a six member ring, cyclo(trimmido-hexamethyltrigallium), with the release of one methane molecule per Ga atom. The overall reaction proceeds in two steps, as indicated by EQNS (2) and (3). The first step is methane elimination to form $(CH_3)_2Ga{:}NH_2$, followed by the oligomerisation of this compound.

$$(CH_3)_3Ga{:}NH_3 \rightarrow (CH_3)_2Ga{:}NH_2 + CH_4 \qquad (2)$$

$$3[(CH_3)_2Ga{:}NH_2] \rightarrow [(CH_3)_2Ga{:}NH_2]_3 \qquad (3)$$

The high temperature gas phase reactions between TMGa and NH_3 have been studied by Thon and Kuech [63] using in situ mass spectroscopy analysis within an isothermal flow tube reactor. H_2 and D_2 were used as the carrier gas and the reactants were mixed at elevated temperature (>200°C) at the inlet of the reactor in order to avoid unintentional low temperature adduct formation. The decomposition of TMGa in both H_2 and H_2/ND_3 is shown in FIGURE 5. Methane (CH_4) is the primary decomposition product of TMGa in an H_2 carrier gas, as shown in FIGURE 5(a). When TMGa is decomposed in the presence of ND_3 and H_2, FIGURE 5(b), there is an immediate reaction between TMGa and ND_3 resulting in the elimination of a single CH_3D molecule at temperatures <500°C. Additional CH_3D molecules are evolved with further decomposition of the TMGa species above 500°C. Based on these results, TMGa and NH_3 are assumed to react at collision rates to form $(CH_3)_2Ga{:}NH_2$ as shown in EQN (4):

$$(CH_3)_3Ga + NH_3 \rightarrow (CH_3)_2Ga{:}NH_2 + CH_4 \qquad (4)$$

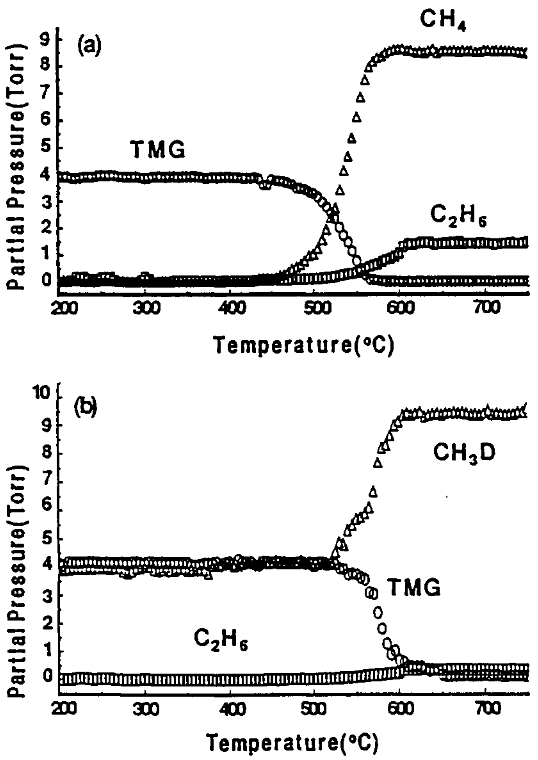

FIGURE 5 Temperature dependence of decomposition for (a) TMG/H_2 and (b) TMG/H_2/ND_3. Immediate reaction between TMG and ND_3 results in the elimination of a single CH_3D molecule [63].

Formation of the dimeric or trimeric compounds, similar to that described in EQN (3), is expected to occur.

The gas phase decomposition results indicate that at typical MOVPE growth conditions, very little if any $(CH_3)_3Ga$ exists in the gas phase and that the primary Ga-containing precursor within the growth environment is $[(CH_3)_2Ga:NH_2]_x$ $(x < 3)$. The GaN growth rate and growth rate uniformity in a given MOVPE reactor geometry are therefore likely to be determined by diffusion and further reactions of this species.

D DETAILED GROWTH MODEL

Two and three dimensional transport models have been used to gain insight into the effects of reactor geometry, flow conditions and carrier gas on the velocity and thermal profiles in a MOVPE reactor. Transport models of GaN growth have been reported by several groups [21-23,64,65]. These models involve the simultaneous solution of non-linear, coupled partial differential equations representing the conservation of momentum, energy, total mass and individual species assuming appropriate boundary conditions. In modelling the growth of GaAs, both TMGa and AsH_3 are assumed to be dilute and the gas phase properties are determined by the H_2 carrier gas alone. In contrast, NH_3 is present in high concentrations in the GaN growth environment and the gas phase properties depend on the mixture of NH_3 and carrier gas (H_2 or N_2) used in the growth process.

Transport modelling provides useful insights into the effects of reactor geometry and growth conditions on the velocity, thermal and concentration profiles in the reactor. In a typical GaN MOVPE reactor, large temperature gradients exist between the cooled walls of the reactor and the high temperature substrate. The high thermal gradients combined with complex split flow inlet geometries and high gas velocities can lead to undesired recirculations in the reactor depending on flow conditions.

It is common practice to vary the carrier gas from H_2 to N_2 during the growth of AlGaN/InGaN heterostructures. The physical properties of H_2 and N_2 are significantly different, however, and consequently the flow profiles in the reactor may vary during growth unless process conditions are adjusted accordingly. The density of N_2 is higher, and the dynamic viscosity, heat conductivity and specific heat capacity are lower than those of H_2. As a result, using N_2 results in higher Reynolds numbers compared to H_2 for a given set of process conditions. In order to maintain a constant Reynolds number and therefore a constant flow profile in the reactor, a higher flow rate of H_2 must be used compared to N_2.

Incorporating an apparent chemistry model of GaN into a two-dimensional transport model, Safvi et al [22] predicted GaN growth rate and growth rate uniformity in a vertical reactor. The inlet geometry of the reactor used in this study consisted of two concentric tubes with the group III and group V species being introduced into the reactor through the inner and outer annular regions, respectively. The apparent chemistry model incorporates in a parametric fashion the three salient features of GaN MOVPE: growth limited by mass transport, contributions to the growth rate from the decomposition of monomer and/or some adduct reaction product, and the loss of nutrients by parasitic gas phase reactions leading to a reduction in the local growth rate. Included in the apparent chemistry model are the individual decomposition reactions of TMGa [66] as well as the gas phase reactions between TMGa and NH_3 (EQNS (3) and (4)). The growth rate of GaN was assumed to be determined by the flux of Ga-containing species to the surface.

The GaN growth rate across the radius of the substrate was calculated using two different assumptions: (A) no loss of growth reactants due to gas phase parasitic reactions, and (B) with parasitic gas phase reactions and growth occurring primarily via the decomposition of the cyclic compound $[(CH_3)_3Ga:NH_2]_3$. Two different flow rates for hydrogen through the inner tube carrying the group III compounds were examined: 5 slm and 0.2 slm of hydrogen. High hydrogen flow rates through the group III inlet tube reduce the gas phase residence time of Ga containing compounds and therefore reduce the loss of Ga species due to parasitic reaction. All other growth conditions including the total flow rate in the reactor were kept constant.

The growth rate of GaN versus radial distance for the high flow (5 slm) and low flow (0.2 slm) cases are shown in FIGURES 6(a) and 6(b), respectively. Also plotted with the data are growth rate predictions for assumptions A and B. In the high flow case, FIGURE 6(a), the growth rate uniformity is poor and the growth rate decreases by almost a factor of 4 from the centre of the substrate to the edge. The experimental growth rate at the centre of the substrate is intermediate between the two extremes predicted by the model. In the low flow case, FIGURE 6(b), the growth rate uniformity across the substrate has improved due to increased gas phase mixing; however the overall growth rate is reduced compared to the high flow conditions. The experimental growth rate at the centre of the substrate for the low flow case is close to that predicted by assumption B. Increased gas residence times increase the extent of parasitic reactions leading to a reduction in the GaN growth rate.

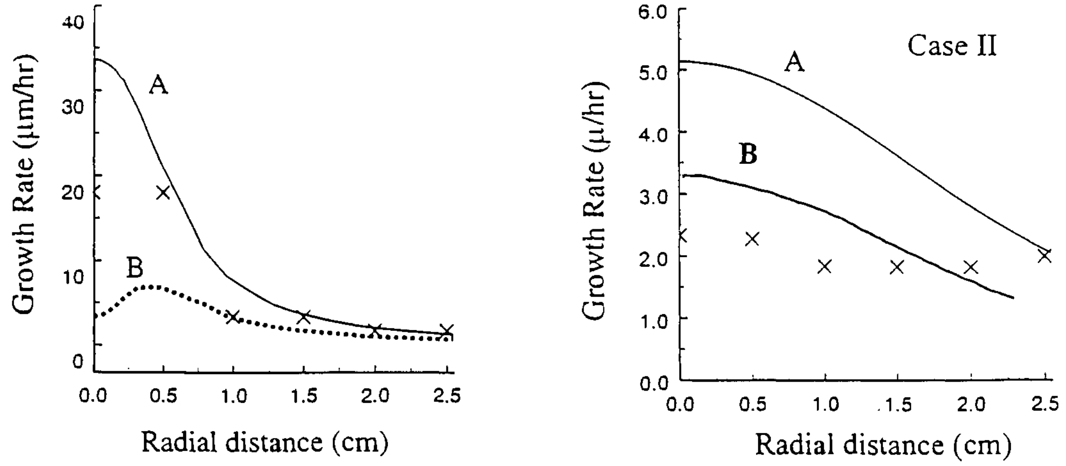

FIGURE 6 Plot of growth rate (μm/hr) along substrate under process conditions of (a) case I (high flow rate) and (b) case II (low flow rate) [22]. Curve A corresponds to ideal growth assuming no parasitic reactions occur. Curve B corresponds to growth from the cyclic compound if all available inlet TMGa converts to the cyclic compound. The simulation predictions are compared to the experimentally measured data (x).

E SUMMARY AND CONCLUSION

The MOVPE growth technique has been used extensively for the fabrication of group III nitride heterostructures and devices. Recent studies have contributed significantly to the current understanding of chemistry and transport processes which govern the GaN MOVPE growth process. GaN growth is limited by mass transport over a fairly wide range of temperatures, similar to MOVPE growth of GaAs. The gas phase and surface chemistry of GaN growth, however, are very complex. Gas phase reactions between TMGa and NH_3 occur at collision rates under typical MOVPE conditions leading to the formation of adducts and cyclic compounds. As a result, the growth rate and quality of GaN are strongly dependent on reactor geometry and flow conditions. Chemical and transport models of GaN growth in a specific reactor geometry are useful for optimising flow conditions and growth rate uniformity.

The MOVPE growth chemistries of AlGaN and InGaN alloys are more complex than that of GaN. The growth of AlGaN alloys appears to be controlled by gas phase chemistry. Gas phase pre-reactions which occur between TMAl and NH_3 reduce the growth efficiency of AlGaN and result in a strong dependence of growth rate and composition on reactor geometry, total pressure and gas phase residence time. InGaN growth, on the other hand, is strongly dependent on growth temperature, growth rate and carrier gas type, indicative of a process that is controlled by surface kinetics.

REFERENCES

[1] H.M. Manasevit, F.M. Erdmann, W.I. Simpson [*J. Electrochem. Soc. (USA)* vol.118 (1971) p.1864-8]

[2] Y. Morimoto, K. Uchiho, S. Ushio [*J. Electrochem. Soc. (USA)* vol.120 (1973) p.1783-5]

[3] T. Sasaki, S. Zembutsu [*J. Appl. Phys. (USA)* vol.61 (1987) p.2533-40]

[4] B.B. Kosicki, D. Kahng [*J. Vac. Sci. Technol. (USA)* vol.6 (1969) p.593-6]

[5] H. Amano, N. Sawaki, I. Akasaki, Y. Toyoda [*Appl. Phys. Lett. (USA)* vol.48 (1986) p.353-5]

[6] S. Nakamura [*Jpn. J. Appl. Phys. (Japan)* vol.30 (1991) p.L1705-7]

[7] H. Amano, M. Kito, K. Hiramatsu, I. Akasaki [*Jpn. J. Appl. Phys. (Japan)* vol.28 (1989) p.L2112-4]

[8] S. Nakamura, N. Iwasa, M. Senoh, T. Mukai [*Jpn. J. Appl. Phys. (Japan)* vol.31 (1992) p.1258-66]

[9] K. Ito, K. Hiramatsu, H. Amano, I. Akasaki [*J. Cryst. Growth (Netherlands)* vol.104 (1990) p.533-8]

[10] S. Nakamura, T. Mukai [*Jpn. J. Appl. Phys. (Japan)* vol.31 (1992) p.L1457-9]

[11] M.A. Khan, R.A. Skogman, J.M. Van Hove, S. Krishnanakutty, R.M. Kolbas [*Appl. Phys. Lett. (USA)* vol.56 (1990) p.1257-9]

[12] S. Nakamura et al [*Appl. Phys. Lett. (USA)* vol.64 (1994) p.1687-9]

[13] S. Nakamura et al [*Appl. Phys. Lett. (USA)* vol.68 (1996) p.2105-7]

[14] R.H. Moss [*J. Cryst. Growth (Netherlands)* vol.68 (1984) p.78-82]

[15] D. Mazzarese, A. Tripathi, W.C. Conner, K.A. Jones, L. Calderon, W. Eckart [*J. Electron. Mater. (USA)* vol.18 (1989) p.369-78]

[16] B.S. Sywe, J.R. Schlup, J.H. Edgar [*Chem. Mater. (USA)* vol.3 (1991) p.737-42]

[17] M.J. Almond, C.E. Jenkins, D.A. Rice, K. Hagen [*J. Organomet. Chem. (France)* vol.439 (1992) p.251-61]

[18] B.P. Keller et al [*J. Electron. Mater. (USA)* vol.24 (1995) p.1707-9]

[19] N. Yoshimoto, T. Matsuoka, T. Sasaki, A. Katsui [*Appl. Phys. Lett. (USA)* vol.59 (1991) p.2251-3]

[20] C. Yuan et al [*J. Electron. Mater. (USA)* vol.25 (1996) p.749-53]

[21] S.A. Safvi, J.M. Redwing, M.A. Tischler, T.F. Kuech [*Mater. Res. Soc. Symp. Proc. (USA)* vol.395 (1996) p.255-60]

[22] S.A. Safvi, J.M. Redwing, M.A. Tischler, T.F. Kuech [*J. Electrochem. Soc. (USA)* vol.144 (1997) p.1789-96]

[23] T.G. Mihopoulos, H. Simka, K.F. Jensen, C. Kuo, H. Liu, C. Chen [*Eighth Int. Conf. on Metalorganic Vapour Phase Epitaxy* Cardiff, Wales, UK, 9-13 June 1996, paper OH.6]

[24] R.D. Dupuis [*J. Cryst. Growth (Netherlands)* vol.178 (1997) p.56-73]

[25] S.N. Mohammad, H. Morkoc [*Prog. Quantum Electron. (UK)* vol.20 (1996) p.361-525]

[26] S.P. DenBaars, S. Keller [in *Gallium Nitride Materials and Devices* vol.50 Eds. J. Pankove, T. Moustakas (Academic Press, 1997) p.11-37]

[27] G.B. Stringfellow [*Organometallic Vapor Phase Epitaxy: Theory and Practice* (Associated Press, San Diego, 1989) p.10]

[28] C.H. Chen et al [*J. Electron. Mater. (USA)* vol.25 (1996) p.1004-8]

[29] T. Detchprohm, K. Hiramatsu, N. Sawaki, I. Akasaki [*J. Cryst. Growth (Netherlands)* vol.137 (1994) p.170-4]

[30] S. Nakamura, T. Mukai, M. Senoh [*Jpn. J. Appl. Phys. (Japan)* vol.32 (1993) p.L16-9]

[31] S. Nakamura, Y. Harada, M. Seno [*Appl. Phys. Lett. (USA)* vol.58 (1991) p.2021-3]

[32] R.F. Davis et al [*Mater. Res. Soc. Symp. Proc. (USA)* vol.395 (1996) p.3-13]

[33] W. Qian, M. Skowronski, M. De Graef, K. Doverspike, L.B. Rowland, D.K. Gaskill [*Appl. Phys. Lett. (USA)* vol.66 (1995) p.1252-4]

[34] K.G. Fertitta, A.L. Holmes, J.G. Neff, F.J. Ciuba, R.D. Dupuis [*Appl. Phys. Lett. (USA)* vol.65 (1994) p.1823-5]

[35] J.M. Redwing, J.S. Flynn, M.A. Tischler, D.A.S. Loeber, N.G. Anderson [*Mater. Res. Soc. Fall Meeting* Boston, MA (1995) paper AAA3.19]

[36] D.K. Wickenden, C.B. Bargeron, W.A. Bryden, J. Miragliotta, T.J. Kistenmacher [*Appl. Phys. Lett. (USA)* vol.65 (1994) p.2024-6]

[37] B.W. Lim, Q.C. Chen, J.Y. Yang, M.A. Khan [*Appl. Phys. Lett. (USA)* vol.68 (1996) p.3761-2]

[38] Z.J. Yu, B.S. Sywe, A.U. Ahmed, J.H. Edgar [*J. Electron. Mater. (USA)* vol.21 (1992) p.383-7]

[39] D.H. Reep, S.K. Ghandi [*J. Electrochem. Soc. (USA)* vol.130 (1983) p.675-80]

[40] R. Niebuhr, K. Bachem, K. Dombrowski, M. Maier, W. Pletschen, U. Kaufman [*J. Electron. Mater. (USA)* vol.24 (1995) p.1531-4]

[41] O. Briot, J.P. Alexis, B. Gil, R.L. Aulombard [*Mater. Res. Soc. Symp. Proc. (USA)* vol.395 (1996) p.207-12]

[42] S. Ruffenach-Clur, O. Briot, B. Gil, R.L. Aulombard [*MRS Internet J. Nitride Semicond. Res. (USA)* vol.2 (1997) article 27]

[43] K. Sayyah, B.C. Chung, M. Gershenzon [*J. Cryst. Growth (Netherlands)* vol.77 (1986) p.424-9]

[44] S. Porowski, J. Jun, P. Perlin, I. Grzegory, H. Teisseyre, T. Suski [*Inst. Phys. Conf. Ser. (UK)* no.173 (1993) p.369-72]

[45] T. Matsuoka, H. Tanaka, T. Sasaki, A. Katsui [*Inst. Phys. Conf. Ser. (UK)* no.106 (1989) p.141-6]

[46] T. Matsuoka, N. Yoshimoto, T. Sasaki, A. Katsui [*J. Electron. Mater. (USA)* vol.21 (1992) p.157-63]

[47] S. Keller et al [*Appl. Phys. Lett. (USA)* vol.68 1996) p.3147-9]

[48] S.M. Bedair, F.G. McIntosh, J.C. Roberts, E.L. Piner, K.S. Boutros, N.A. El-Masry [*J. Cryst. Growth (Netherlands)* vol.178 (1997) p.32-44]

[49] E.L. Piner et al [*Appl. Phys. Lett. (USA)* vol.70 (1997) p.461-3]

[50] J. Han, T.B. Ng, R.M. Biefeld, M.H. Crawford, D.M. Follstaedt [*Appl. Phys. Lett. (USA)* vol.71 (1997) p.3114-6]

[51] M. Hashimoto, H. Amano, N. Sawaki, I. Akasaki [*J. Cryst. Growth (Netherlands)* vol.68 (1984) p.163]

[52] J. Han, J.J. Figiel, M.H. Crawford, R.M. Biefeld [*Int. Conf. Metalorganic Vapor Phase Epitaxy IX* La Jolla, CA, USA, 31 May-4 June 1998]

[53] I. Ho, G.B. Stringfellow [*Appl. Phys. Lett. (USA)* vol.69 (1996) p.2701-3]

[54] M.D. McCluskey, L.T. Romano, B.S. Krusor, D.P. Bour, S. Brennan [*Appl. Phys. Lett. (USA)* vol.72 (1998) p.1730-2]

[55] R. Singh, D. Doppalapudi, T.D. Moustakas, L.T. Romano [*Appl. Phys. Lett. (USA)* vol.70 (1997) p.1089-91]

[56] S.P. DenBaars, B.Y. Maa, P.D. Dapkus, A.D. Danner, H.C. Lee [*J. Cryst. Growth (Netherlands)* vol.77 (1986) p.188-93]

[57] C.A. Larson, N.I. Buchan, S.H. Li, G.B. Stringfellow [*J. Cryst. Growth (Netherlands)* vol.102 (1990) p.103-16]

[58] [*NIST Database 17* (NIST Chemical Kinetics, U.S. Department of Commerce, National Institute of Standards and Technology, 1994) and references therein]

[59] M. Kamp et al [*Mater. Res. Soc. Symp. Proc. (USA)* vol.395 (1996) p.135-9]

[60] G.E. Coates [*J. Chem. Soc. Part III (UK)* (1951) p.2003-8]

[61] A. Zaouk, E. Salvetat, J. Sakaya, F. Maury, G. Constant [*J. Cryst. Growth (Netherlands)* vol.55 (1981) p.135-44]

[62] M.J. Almond, M.G.B. Drew, C.E. Jenkins, D.A. Rice [*J. Chem. Soc., Dalton Trans. (UK)* iss.1 (1992) p.5-9]

[63] A. Thon, T.F. Kuech [*Appl. Phys. Lett. (USA)* vol.69 (1996) p.55-7]

[64] H. Jurgensen et al [*MRS Internet J. Nitride Semicond. Res. (USA)* vol.1 (1996) article 26]

[65] C. Theodoropoulos, H.K. Moffat, T.J. Mountziaris [*Int. Conf. Metalorganic Vapor Phase Epitaxy IX* La Jolla, CA, USA, 31 May-4 June 1998]

[66] M.J. Jacko, S.W. Price [*Can. J. Chem. (Canada)* vol.41 (1963) p.1560-6]